

Linköping University Post Print

Relating the open-circuit voltage to interface molecular properties of donor:acceptor bulk heterojunction solar cells

Koen Vandewal, Kristofer Tvingstedt, Abay Gadisa, Olle Inganäs and Jean V Manca

N.B.: When citing this work, cite the original article.

Original Publication:

Koen Vandewal, Kristofer Tvingstedt, Abay Gadisa, Olle Inganäs and Jean V Manca, Relating the open-circuit voltage to interface molecular properties of donor:acceptor bulk heterojunction solar cells, 2010, PHYSICAL REVIEW B, (81), 12, 125204.

<http://dx.doi.org/10.1103/PhysRevB.81.125204>

Copyright: American Physical Society

<http://www.aps.org/>

Postprint available at: Linköping University Electronic Press

<http://urn.kb.se/resolve?urn=urn:nbn:se:liu:diva-54852>

Relating the open-circuit voltage to interface molecular properties of donor:acceptor bulk heterojunction solar cells

Koen Vandewal,^{1,*} Kristofer Tvingstedt,² Abay Gadisa,¹ Olle Inganäs,² and Jean V. Manca¹

¹IMEC-IMOMEC, vzw and Institute for Materials Research, Hasselt University, Wetenschapspark 1, 3590 Diepenbeek, Belgium

²Biomolecular and Organic Electronics, Center of Organic Electronics (COE), Department of Physics, Chemistry and Biology, Linköping University, 58183 Linköping, Sweden

(Received 18 September 2009; revised manuscript received 3 February 2010; published 10 March 2010)

The open-circuit voltage (V_{oc}) of polymer:fullerene bulk heterojunction solar cells is determined by the interfacial charge-transfer (CT) states between polymer and fullerene. Fourier-transform photocurrent spectroscopy and electroluminescence spectra of several polymer:fullerene blends are used to extract the relevant interfacial molecular parameters. An analytical expression linking these properties to V_{oc} is deduced and shown to be valid for photovoltaic devices comprising three commonly used conjugated polymers blended with the fullerene derivative [6,6]-phenyl-C61-butyric acid methyl ester (PCBM). V_{oc} is proportional to the energy of the CT states E_{CT} . The energetic loss $q\Delta V$ between E_{CT} and qV_{oc} vanishes when approaching 0 K. It depends linearly on T and logarithmically on illumination intensity. Furthermore $q\Delta V$ can be reduced by decreasing the electronic coupling between polymer and fullerene or by reducing the nonradiative recombination rate. For the investigated devices we find a loss $q\Delta V$ of ~ 0.6 eV at room temperature and under solar illumination conditions, of which ~ 0.25 eV is due to radiative recombination via the CT state and ~ 0.35 eV is due to nonradiative recombination.

DOI: [10.1103/PhysRevB.81.125204](https://doi.org/10.1103/PhysRevB.81.125204)

PACS number(s): 71.35.Gg, 72.40.+w, 72.80.Rj, 73.50.Pz

I. INTRODUCTION

Research in organic photovoltaics has advanced over the recent years. Currently power conversion efficiencies of 5% to above 7%, with external quantum efficiencies of 70–80% (Refs. 1–5) and internal quantum efficiencies approaching 100%, are achieved for polymer:fullerene photovoltaic devices. This indicates that in these high quantum efficiency cases, nearly all photons absorbed by the polymer are converted into collected electrons at short circuit and, hence, that the achieved short-circuit currents are close to their predicted maximum. Power conversion efficiency, however, does not only depend on the production of photocurrent but also on the photovoltage. Optimization and understanding of the fundamental limits of the open-circuit voltage (V_{oc}) therefore are as important as the optimization of the short-circuit current (J_{sc}).

V_{oc} has been shown to depend on the donor/acceptor material combination,^{6,7} the electrode material,⁸ as well as light intensity and temperature.⁹ Modeling of the internal field and charge distribution has successfully explained the influence of several of these parameters on V_{oc} . However, there exists also a relation between externally measurable electro-optical spectra and V_{oc} .¹⁰ This relation is based on the principle of detailed balance and the assumption of quasiequilibrium conditions.^{11,12} A benefit of this approach is that it avoids description of the internal charge and field distributions in the solar cell, which are difficult to measure. With this theory, the origin of V_{oc} of polymer:fullerene solar cells can be explained in terms of ground-state charge-transfer complex (CTC) formation between polymer and fullerene.¹⁰

Upon blending a suitable donor polymer with a fullerene acceptor, interaction between polymer and fullerene results in the formation of a ground-state CTC.^{13–22} Upon excitation of this new ground state, the CT exciton is created. Optical

transitions from the CTC ground state to the CT exciton are visible in the low-energy region of the photovoltaic external quantum efficiency (EQE_{PV}) spectrum if measured with sensitive techniques.¹⁸ Radiative decay of CT excitons is sometimes observed in photoluminescence measurements of polymer:fullerene blends^{14–16,19–22} and can be more easily detected in electroluminescence (EL) spectra obtained by applying a forward voltage over polymer:fullerene photovoltaic devices.²¹

CT excitons play a major role in the operation of polymer:fullerene solar cells.^{10,14,19,22} These weakly bound electron-hole pairs at the polymer:fullerene interface are mainly populated via a photoinduced electron transfer after excitation of polymer or fullerene. Due to the low oscillator strength of polymer:fullerene CTCs only a very small fraction of CT excitons is populated by direct optical excitation of the CTCs. The major contribution to the photocurrent originates from polymer or fullerene excitation. However, the efficiency of CT exciton formation and their dissociation into free carriers determines the photocurrent.^{14,19,22} Both formation and dissociation efficiencies depend on the blend morphology and donor:acceptor energetics. Also V_{oc} is determined by the spectral properties of the CT excitons, again being morphology dependent. In general, the spectral position of the CT exciton correlates with the difference between the lowest unoccupied molecular orbital (LUMO) of the fullerene acceptor and the highest occupied molecular orbital (HOMO) of the donor polymer,²³ resulting in the widely observed correlation between V_{oc} and this difference.^{1,2,6,7} However, recently it has been argued that other CTC related parameters, such as the electronic coupling between donor and acceptor, also have an influence on V_{oc} .^{24,25}

In this paper we aim to describe in more detail how V_{oc} is affected by CTC properties. These properties are obtained by observing the CT optical transition bands in sensitive mea-

measurements of the photovoltaic external quantum efficiency (EQE_{PV}) spectrum and the EL spectrum. An analytical expression for V_{oc} as a function of interfacial CTC properties is deduced. V_{oc} is shown to be proportional to the energy of the interfacial CT state E_{CT} . The energetic loss between E_{CT} and qV_{oc} depends linearly on temperature and logarithmically on illumination intensity as observed also by others.^{9,26} In this work we show that this loss can be reduced by reducing the electronic coupling between polymer and fullerene and by reducing the nonradiative recombination.

The derived analytical expression is shown to be valid in a temperature range from 150 to 300 K and under different illumination intensities, for four material systems, consisting of poly[2-methoxy-5-(30,70-dimethyloctyloxy)-1,4-phenylene vinylene] (MDMO-PPV), poly[3-hexylthiophene] (P3HT), and poly[2,7-(9-di-octyl-fluorene)-alt-5,5-(4',7'-di-2-thienyl-2',1',3'-benzothiadiazole)] (APFO3), blended with the fullerene derivative [6,6]-Phenyl C61 butyric acid Methyl ester (PCBM). For the APFO3 based devices, APFO3:PCBM 1:4 and 1:1 stoichiometries were studied.

II. THEORY

In the framework of Marcus theory, the spectral lineshape of the CT absorption cross section $\sigma(E)$ at photon energy E is described by^{27,28}

$$\sigma(E)E = \frac{f_{\sigma}}{\sqrt{4\pi\lambda kT}} \exp\left(\frac{-(E_{CT} + \lambda - E)^2}{4\lambda kT}\right) \quad (1)$$

Hereby is k Boltzmann's constant and T is the absolute temperature. E_{CT} is the free-energy difference between the CTC ground state and the CT excited state and λ is a reorganization energy associated with the CT absorption process, as shown in Fig. 1(a). f_{σ} does not depend on E (Ref. 28) and is proportional to the square of the electronic coupling matrix element. It represents a measure of the strength of the donor/acceptor material interaction. The absorption coefficient α in the spectral region of CT absorption equals σN_{CTC} , with N_{CTC} as the number of CTCs per unit volume.

The emission rate I_f at photon energy E , per unit energy equals^{27,28}

$$\frac{I_f}{E} = \frac{f_{I_f}}{\sqrt{4\pi\lambda kT}} \exp\left(\frac{-(E_{CT} - \lambda - E)^2}{4\lambda kT}\right). \quad (2)$$

In analogy to f_{σ} , f_{I_f} is not dependent on E and is proportional to the square of the electronic coupling matrix element.²⁸ The left-hand side of Eqs. (1) and (2) are called the reduced absorption and emission spectrum, respectively. They exhibit a mirror image relationship. The midpoint energy of these two spectra equals E_{CT} . In principle, λ can be deduced from the Stokes shift, or from the linewidth of the absorption or emission bands, by fitting with formulas (1) or (2). This is visualized in the scheme shown in Fig. 1(a). It should be noted however that in real materials, the Stokes shift can differ from 2λ as a result of a disordered density of states, with emission taking place only from the lower-energy excited states.²⁹

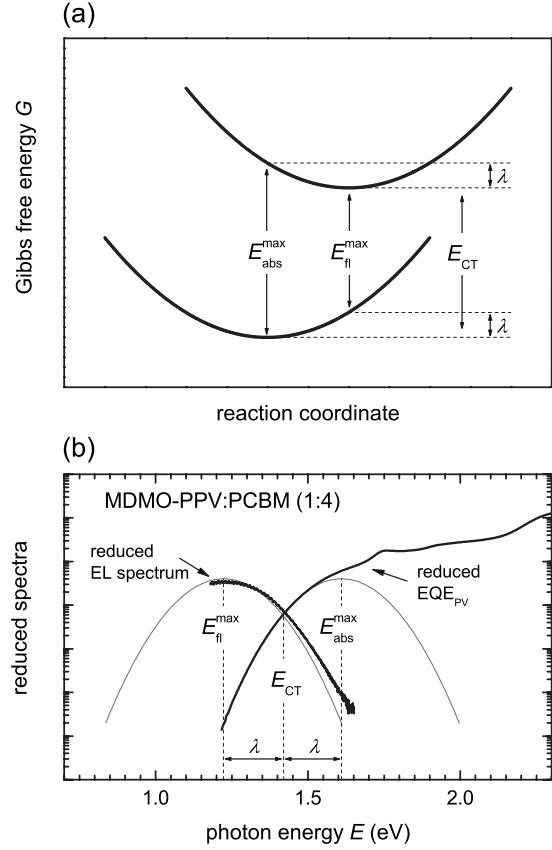


FIG. 1. (a) Free-energy diagram for the ground state and lowest excited state of the CTC as a function of a generalized coordinate. (b) Reduced EQE_{PV} and EL spectrum for a MDMO-PPV:PCBM (1:4) photovoltaic device. The gray curves are fits of the EQE_{PV} and EL spectra using formulas (1) and (2), using the same E_{CT} and λ values. These parameters, together with the maxima of absorption E_{abs}^{max} and emission E_{fl}^{max} , are indicated in the figure.

Because of their low absorption coefficients, highly sensitive techniques are needed to spectrally resolve CT absorption bands in polymer:fullerene blends.³⁰ We use Fourier-transform photocurrent spectroscopy (FTPS) to measure the photovoltaic EQE_{PV} spectrum of polymer:fullerene devices over several decades. The CT bands are visible in the low-energy part of the EQE_{PV} spectrum. Because of the low value of α , the total absorption in this spectral region can be approximated by $\alpha 2d$, when using a back reflecting metal cathode. The EQE_{PV} equals the total absorption $\alpha 2d$, multiplied by the absorbed-photon-to-electron internal-conversion efficiency η ,

$$EQE_{PV}(E) = \eta \sigma(E) N_{CTC} 2d. \quad (3)$$

Using Eq. (1) for $\sigma(E)$ we obtain in the spectral region of CT absorption,

$$EQE_{PV}(E) = \frac{f}{E \sqrt{4\pi\lambda kT}} \exp\left(\frac{-(E_{CT} + \lambda - E)^2}{4\lambda kT}\right) \quad (4)$$

In this equation the prefactor f equals $\eta N_{CTC} 2d f_{\sigma}$. The normalized reduced EQE_{PV} and EL emission spectra are shown in Fig. 1(b) for MDMO-PPV:PCBM in a 1:4 ratio. In

the figure we have indicated how the parameters E_{CT} and λ in Fig. 1(a) can be deduced from Fig. 1(b).

We will now relate these CTC properties to V_{oc} . In Ref. 10, using the method of detailed balance we have shown that the CT states relate to the dark current and V_{oc} . The following expression for the dark injected current J_{inj} versus voltage characteristic was used, with q being the elementary charge:

$$J_{inj} = J_0 \left[\exp\left(\frac{qV}{kT}\right) - 1 \right]. \quad (5)$$

Hereby is implicitly assumed that J_0 can still depend on the applied voltage or charge density present in the device. For the P3HT:PCBM material system, Shuttle *et al.* showed that, for voltages smaller or comparable to V_{oc} , this dark injected current J_{inj} constitutes recombination current only.³¹ At V_{oc} , this recombination current balances with the photo-generated current J_{ph} , and V_{oc} is given by

$$V_{oc} = \frac{kT}{q} \ln\left(\frac{J_{ph}}{J_0} + 1\right) \quad (6)$$

Following the reasoning of Rau,¹² J_0 is related to the electro-optical properties by

$$J_0 = \frac{q}{EQE_{EL}} \int EQE_{PV}(E) \phi_{BB}^T dE \quad (7)$$

Hereby is EQE_{EL} the EL external quantum efficiency and ϕ_{BB}^T is the black body spectrum at temperature T . If in this expression [Eq. (7)], EQE_{PV} is evaluated at short circuit, J_{ph} in expression (6) should also be evaluated at short circuit using $J_{ph} = J_{sc}$ in the evaluation of that equation.¹⁰

Further is the integral of the product $\phi_{BB}^T EQE_{PV}$ of importance. Because ϕ_{BB}^T is strongly decreasing with increasing energy, only the low-energy CT part of the EQE_{PV} spectrum contributes to this integral.¹⁰ Using formula (4) in formula (7) gives

$$J_0 \approx \frac{q}{EQE_{EL}} f \frac{2\pi}{h^3 c^2} (E_{CT} - \lambda) \exp\left(-\frac{E_{CT}}{kT}\right). \quad (8)$$

The derivation of Eq. (8) is explained in more detail in the Appendix. From Eqs. (6) and (8) and with $J_{ph} = J_{sc}$, we get an analytical expression for V_{oc} as a function of EQE_{EL} and the parameters E_{CT} , λ and f , evaluated at short circuit,

$$V_{oc} = \frac{E_{CT}}{q} + \frac{kT}{q} \ln\left(\frac{J_{sc} h^3 c^2}{f q 2\pi (E_{CT} - \lambda)}\right) + \frac{kT}{q} \ln(EQE_{EL}). \quad (9)$$

This formula implies a linear dependence of V_{oc} on temperature and a logarithmic dependence on illumination intensity. Such dependencies are observed and described in the literature.^{9,32,33} The formulation of Eq. (9) however allows us to relate measurable properties related to the molecular interface between donor and acceptor to V_{oc} . This will be further discussed in the next sections.

III. EXTRACTION OF CTC PROPERTIES

We have investigated polymer:PCBM solar cells based on three different donor polymers, i.e., MDMO-PPV, P3HT,

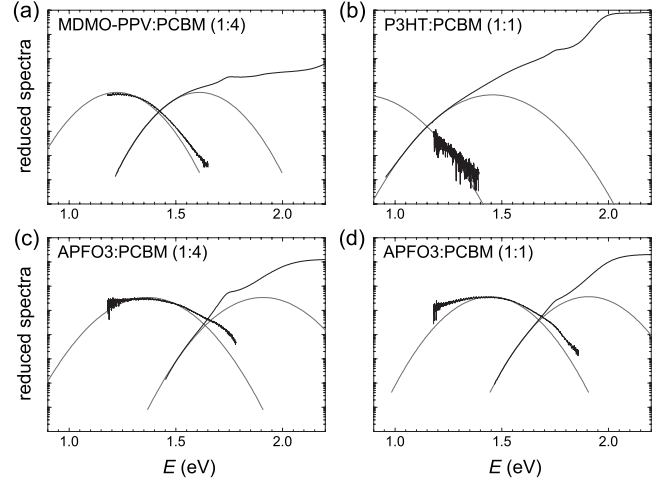


FIG. 2. Reduced EQE_{PV} and EL spectrum for (a) APFO3:PCBM (1:4), (b) APFO3:PCBM (1:1), and P3HT:PCBM (1:1) photovoltaic devices measured at room temperature. The gray curves are fits of the EQE_{PV} and EL spectra using formulas (1) and (2), with the same values for E_{CT} and λ .

APFO3. For the APFO3:PCBM blends, the polymer:fullerene 1:1 and 1:4 weight ratios are investigated. The EQE_{PV} and EL spectrum of MDMO-PPV:PCBM in a 1:4 ratio were already shown in Fig. 1(b). The spectra for the APFO3 and P3HT based devices are shown in Fig. 2.

For all material systems, we can deduce the reorganization energy λ and E_{CT} by fitting the CT band in the EQE_{PV} spectrum with Eq. (4). The EL emission spectra were measured with the aid of a Si charge couple device camera in the spectral range above 1.2 eV. In this range, the shape of the predicted reduced emission spectrum calculated via formula (2) resembles the measured reduced EL spectrum for all devices. The observed deviations from the predicted emission spectrum and the measured one are probably due to an increased effective temperature upon injecting current. Also effects related to a disordered density of states may contribute. However, we can conclude that the spectral shape of the CT bands at room temperature can be described to a fairly good approximation with formulas (1)–(4).

We have also applied formula (4) to account for the temperature dependence of the CT band. EQE_{PV} spectra were obtained between 150 and 300 K. The spectra for the four different material systems are shown in Fig. 3, together with their fits using formula (4). The obtained parameters are listed in Table I. The APFO3:PCBM blends show the highest E_{CT} , with the 1:1 stoichiometry having a slightly higher value than the 1:4 stoichiometry. The P3HT:PCBM blend has the lowest E_{CT} (Table I). For all studied material systems, we obtain λ values, which are quite independent of temperature, in the order of 0.2–0.3 eV. The values of E_{CT} , and the values of E_{abs}^{max} however, are slightly temperature dependent. We observe a small redshift of the CT band ~ 0.1 eV upon cooling from 300 to 150 K. The exact origin of this phenomenon is not understood yet but corresponds to what is observed for the temperature dependence of the optical gap of pure conjugated polymers^{34,35} or conjugated polymers involved in a

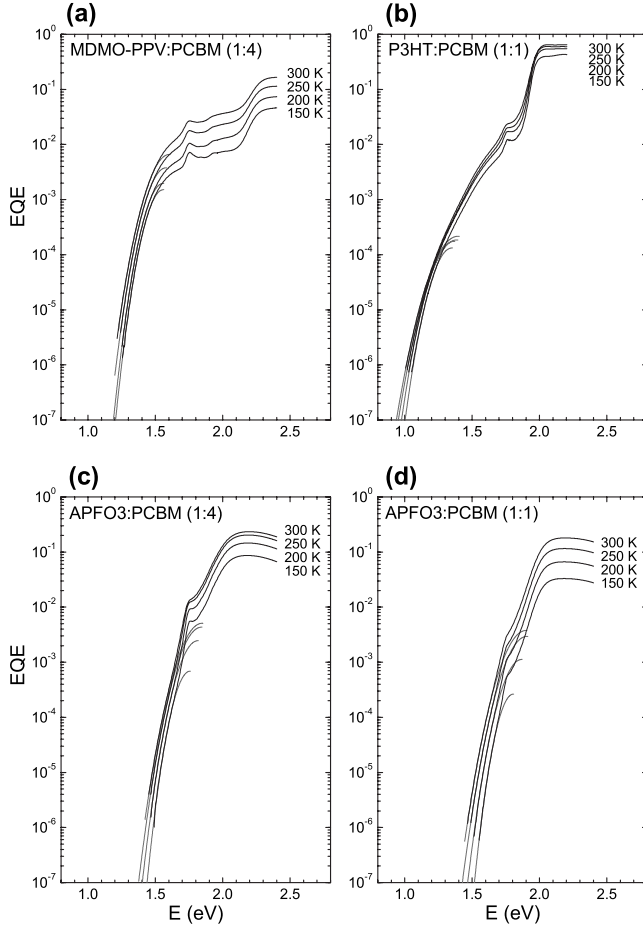


FIG. 3. EQE_{PV} spectra of (a) MDMO-PPV:PCBM (1:4), (b) P3HT:PCBM (1:1), (c) APFO3:PCBM (1:4), and (d) APFO3:PCBM (1:1) measured at several temperatures. The spectra were fitted with formula (4) to obtain values for E_{CT} and λ .

CTC.³⁶ The increase in the optical gap energy of pure materials upon increasing temperature was explained by the presence of an increased disorder at higher temperatures.³⁶

IV. TEMPERATURE DEPENDENCE OF V_{oc}

In this section we investigate the temperature dependence of the dark saturation current J_0 and V_{oc} . We have already seen that E_{CT} also depends on temperature. If we approximate E_{CT} by $E_{CT}^0 + T \frac{dE_{CT}}{dT}$, then, for the investigated devices $\frac{dE_{CT}}{dT}$ is almost constant in the region from ~ 200 to 300 K (Fig. 4). In this case E_{CT}^0 is the intercept of the linear extrapolation of E_{CT} in the 200–300 K region, with the 0 K axis. E_{CT}^0 is also the activation energy of the dark current, for $J_0 \sim \exp(-\frac{E_{CT}^0 + T dE_{CT}/dT}{kT}) \sim \exp(-\frac{E_{CT}^0}{kT})$.

We obtain the following values for E_{CT}^0 : For MDMO-PPV:PCBM (1:4) $E_{CT}^0 = 1.25$ eV and for P3HT:PCBM (1:1) $E_{CT}^0 = 0.94$ eV. These values are very close to the activation energies E_a of the dark saturation current values found in Ref. 32 for MDMO-PPV:PCBM (1:4) ($E_a = 1.25$ eV) and P3HT:PCBM (1:1) ($E_a = 0.92$ eV–0.93 eV). For the APFO3:PCBM (1:4) and APFO3:PCBM (1:1) devices we find, respectively, $E_{CT}^0 = 1.45$ eV and $E_{CT}^0 = 1.51$ eV. This last example indicates that the spectral position of the CT band and E_{CT} are not only affected by the energetic levels of a single donor and a single acceptor molecule but also on polymer:fullerene stoichiometry.¹⁸

Regarding the temperature dependence of V_{oc} , Green (Ref. 37) showed that if the dark recombination current is of the form of Eq. (9), an approximately linear temperature dependence of qV_{oc} is predicted with a 0 K intercept equal to E_{CT}^0 . In Fig. 4, the validity of this reasoning for the four polymer:fullerene solar cells investigated in this work is shown. This figure shows the temperature dependence of the E_{CT} values and V_{oc} values for different illumination intensities, between ~ 0.001 and ~ 0.1 sun. Extrapolation of temperature-dependent values E_{CT} to 0 K coincides very well with the extrapolation of the temperature-dependent V_{oc} for all four material systems and the investigated illumination intensities. For both APFO3 samples, there are some deviations from the straight line at low temperature. For inorganic solar cells, such as Si and GaAs, the same reasoning can be

TABLE I. Summary of the parameters E_{CT} , λ , and f obtained by fitting the CT band in the temperature-dependent EQE_{PV} spectra with Eq. (4).

T (K)	MDMO-PPV:PCBM(1:4)			P3HT:PCBM(1:1)		
	f (eV ²)	E_{CT} (eV)	λ (eV)	f (eV ²)	E_{CT} (eV)	λ (eV)
150	4.8E-4	1.31	0.25	4.1E-5	1.03	0.32
200	6.4E-4	1.36	0.20	6.0E-5	1.08	0.29
250	1.4E-3	1.39	0.19	7.2E-5	1.11	0.29
300	2.6E-3	1.42	0.19	8.8E-5	1.14	0.27
T (K)	APFO3:PCBM(1:4)			APFO3:PCBM(1:1)		
	f (eV ²)	E_{CT} (eV)	λ (eV)	f (eV ²)	E_{CT} (eV)	λ (eV)
150	2.3E-4	1.54	0.22	9.0E-5	1.60	0.20
200	1.0E-3	1.58	0.24	4.9E-4	1.62	0.25
250	2.0E-3	1.61	0.24	1.5E-3	1.65	0.26
300	2.5E-3	1.64	0.21	2.0E-3	1.68	0.23

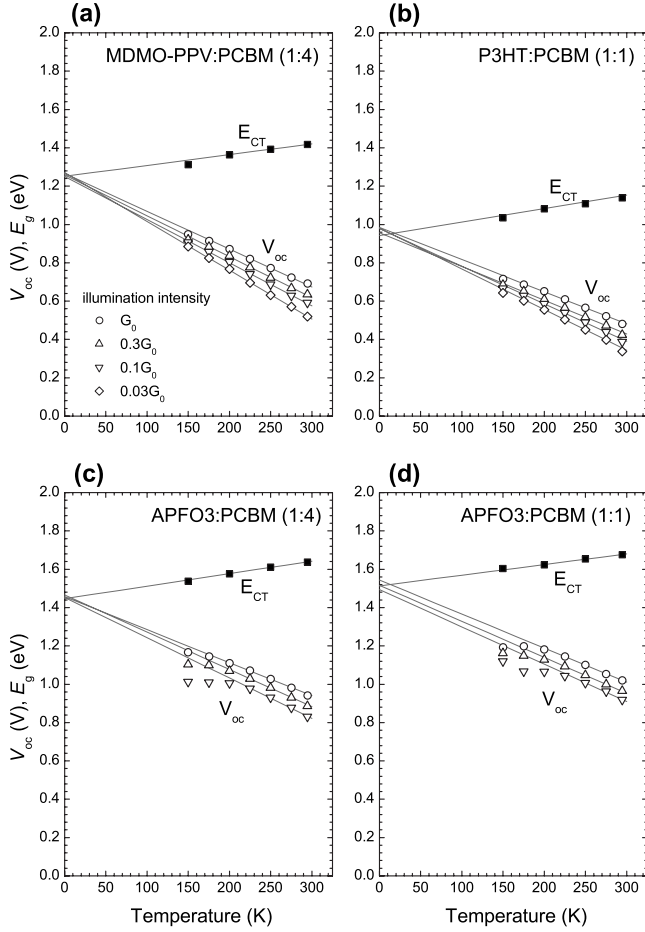


FIG. 4. V_{oc} and E_{CT} in function of temperature. E_{CT} is represented as the filled squares. V_{oc} was measured for different illumination intensities. The highest illumination intensity was G_0 , about 0.1 sun, represented by open circles. The other illumination intensities are $0.3G_0$ (open triangles up), $0.1G_0$ (open triangles down) and $0.03G_0$ (diamonds). E_{CT} and V_{oc} are linearly extrapolated to 0 K in their linear range, from ~ 200 to 300 K. These curves are shown as black lines. Both these extrapolations result in the same value.

made for the relation between V_{oc} and the band gap of the used inorganic material.³⁷ This indicates that, with respect to V_{oc} , the energy of the CT exciton E_{CT} fulfills the same role as the band gap does in inorganic solar cells. This confirms that E_{CT} is an appropriate definition for the gap of organic solar cells based on blends of donor and acceptor materials. Note that E_{CT} is defined differently in this work than it is in previous work,¹⁸ where we used an empirical definition for the interfacial band gap, i.e., the peak energy of the CT band minus two times the width of its Gaussian fit. The effective band gap defined in that work can be related to E_{CT} , as defined in this work as being $4\sqrt{2kT\lambda} - \lambda$ lower. At room temperature and with λ ranging between 0.2–0.3 eV, this makes our previously defined effective band gap ~ 0.2 eV lower than E_{CT} . However we believe that E_{CT} , as defined in the present work, represents the true energy of the CT state rather than the empirically defined effective band gap in Ref. 18 or the peak energy of CT emission.^{19,21}

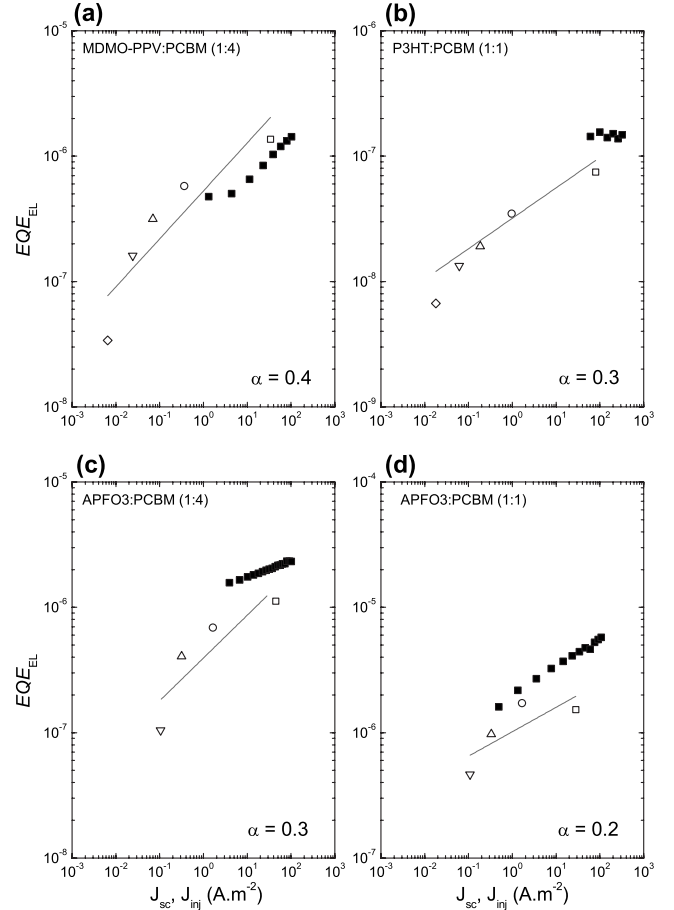


FIG. 5. The calculated and measured EQE_{EL} . The open symbols represent EQE_{EL} versus J_{sc} , calculated from V_{oc} measurements with the aid of formula (9). The filled squares are measurements of EQE_{EL} versus J_{inj} . The full lines represent a power-law dependence of EQE_{EL} on J_{sc} with a power α .

V. ILLUMINATION INTENSITY DEPENDENCE OF V_{oc}

We can calculate EQE_{EL} using expression (9), together with experimentally obtained values for V_{oc} , J_{sc} , E_{CT} , and f . In Fig. 5 the calculated values are shown as a function of the short-circuit current J_{sc} of the device. It can be seen that the calculated EQE_{EL} values are in the order of 10^{-6} to 10^{-9} with the lowest EQE_{EL} values for the P3HT:PCBM (1:1) devices.

In order to compare these calculated EQE_{EL} values with experimental values we have measured EQE_{EL} as a function of injection current, using a Si photodiode. Because of the low EQE_{EL} values, good signals have only been obtained at high injection currents. Because at V_{oc} , the photocurrent and injected current balance, the EQE_{EL} obtained by using formula (9) must be compared with experimentally measured EQE_{EL} at an injection current corresponding to the short-circuit current. In Fig. 5, it can be seen that the experimentally obtained $EQE_{EL}(J_{inj})$ trend corresponds fairly well with the calculated $EQE_{EL}(J_{sc})$.

A dependence of EQE_{EL} on J_{inj} and thus internal charge density is observed. We can approximate the relation of EQE_{EL} as a function of J_{inj} by a power-law relationship

$$EQE_{EL}(J_{inj}) \approx EQE_{EL}(1)J_{inj}^{\alpha}. \quad (10)$$

Hereby is $EQE_{EL}(1)$ the EQE_{EL} measured at an injection current of $1 \text{ A}\cdot\text{m}^{-2}$. This implies that J_0 , as defined in Eq. (8), depends on the number of charges present in the device,

$$J_0(J_{inj}) \approx J_0(1)J_{inj}^{-\alpha}. \quad (11)$$

Hereby does $J_0(1)$ equal J_0 obtained by evaluating Eq. (8) for $EQE_{EL}(1)$. Inserting this expression in Eq. (5) gives for $V \gg \frac{kT}{q}$,

$$J_{inj} = J_{0,n} \exp\left(\frac{qV}{nkT}\right). \quad (12)$$

Hereby $n=1+\alpha$ and $J_{0,n}=[J_0(1)]^{1/n}$. For the material systems investigated in this work, we find values for n between 1 and 1.5.

Using Eq. (12), the expression for $V_{oc} \gg \frac{kT}{q}$ becomes

$$V_{oc} = \frac{nkT}{q} \ln\left(\frac{J_{sc}}{J_{0,n}}\right). \quad (13)$$

In formula (13), $J_{0,n}$ can be considered constant as opposed to J_0 in Eq. (6). Relations of this type including an ideality factor n have been used before to describe the illumination intensity of V_{oc} of organic solar cells.^{9,26,32,33} The factor n finds its origin in the fact that nonradiative recombination mechanisms are present and that these mechanisms depend differently on the charge density or injected current as compared to the radiative recombination mechanism. This causes EQE_{EL} to depend on the injected current. The exact nonradiative recombination mechanisms are not known at present but are currently under investigation. A third-order charge-carrier decay mechanism was found by at least three independent groups.^{38–41} Further elucidation on these polaron recombination mechanisms is of high importance as their reduction will cause an increase in EQE_{EL} and V_{oc} .

VI. VOLTAGE LOSSES IN POLYMER:FULLERENE SOLAR CELLS AT AM1.5 CONDITIONS

We will now do a more detailed study of the energetic losses $q\Delta V$ between qV_{oc} and the gap E_{CT} under solar conditions. In analogy to Ref. 12, this loss can be seen as consisting of two parts, $q\Delta V_{rad}$ and $q\Delta V_{non-rad}$. Equation (9) allows us to calculate these losses,

$$q\Delta V_{rad} = -kT \ln\left(\frac{J_{sc}h^3c^2}{fq2\pi(E_{CT}-\lambda)}\right), \quad (14)$$

$$q\Delta V_{nonrad} = -kT \ln(EQE_{EL}). \quad (15)$$

When all recombination is radiative CT emission, $EQE_{EL}=1$ and ΔV_{nonrad} vanishes. In this case ΔV equals ΔV_{rad} , a loss due solely to radiative emission. It is logarithmically dependent on properties of the CTC and incident light intensity ($\sim J_{sc}$). For a given donor/acceptor pair with fixed E_{CT} , λ , and f , this term is constant and represents a minimum loss between E_{CT} and qV_{oc} for a perfect device in which the only recombination mechanism present is a radiative one. Because of the logarithmical dependence the variation in parameters E_{CT} and λ will not affect this loss much.

TABLE II. Radiative and nonradiative energetic losses at V_{oc} for solar illumination and at room temperature. The radiative losses were calculated from the FTPS spectra. The nonradiative losses are related to EQE_{EL} .

	ΔV (V)	ΔV_{rad} (V)	ΔV_{nonrad} (V)
MDMO-PPV:PCBM (1:4)	0.58	0.24	0.34
P3HT:PCBM (1:1)	0.53	0.11	0.42
APFO3:PCBM (1:4)	0.59	0.24	0.35
APFO3:PCBM (1:1)	0.59	0.25	0.34

However the parameter f can be varied over several decades by varying the electronic coupling between polymer and fullerene. Choosing donor/acceptor pairs with a CT state which has a reduced coupling to the ground state will result in a decreased f and ΔV_{rad} . The question remains if such a reduced coupling is achievable in future material systems without this having a disadvantageous influence on charge transfer and subsequent photocurrent generation.⁴²

The part which takes into account the nonradiative recombination mechanisms, omnipresent in real devices, is reflected in the term ΔV_{nonrad} . This term becomes larger than zero if EQE_{EL} is smaller than unity. As seen above, this part is also logarithmically dependent on J_{sc} , as $EQE_{EL} \sim J_{sc}^\alpha$ for the polymer:fullerene solar cells we have investigated. Similar formulas were derived for the V_{oc} of inorganic solar cells but assumed to be valid for all solar cells operating in quasiequilibrium conditions.³⁷ It is argued that while ΔV_{rad} is a thermodynamically unavoidable loss mechanism for a given material system, ΔV_{nonrad} can in principle be avoided by reducing the nonradiative recombination paths. We experimentally find EQE_{EL} at room temperature in the range from 10^{-9} to 10^{-6} , when using Ca/Al and ITO/PEDOT:PSS contacts. Using non-Ohmic contacts will decrease the value of EQE_{EL} even further. For Si and GaAs solar cells, EQE_{EL} values are in the range of 10^{-3} .³⁷ The question remains if these values can also be achieved for polymer:fullerene solar cells.

In Table II the loss factors are shown for the four investigated devices with ITO/PEDOT:PSS bottom contacts and Ca/Al top contacts under solar conditions. The overall offset ΔV is fairly constant, with a value between 0.5 and 0.6 V. The P3HT:PCBM system has a lower value for f than the other (noncrystalline) polymer:PCBM systems. This results in a lower radiative loss ΔV_{rad} . However in this system, there is no net benefit of this lower ΔV_{rad} because ΔV_{nonrad} is higher as compared to the other material systems. The reason for this higher ΔV_{nonrad} and lower EQE_{EL} in P3HT:PCBM is not clear yet. However, a fairly constant total ΔV is found for all four material systems. This explains the widely observed relation between V_{oc} and the difference between HOMO(D) and LUMO(A) for polymer:fullerene bulk heterojunction solar cells for this difference correlates with E_{CT} .²³

VII. CONCLUSION

In this work, CTC parameters are related to V_{oc} . It was shown that the free-energy difference E_{CT} between excited

CTC and ground state CTC is an appropriate definition of donor:acceptor blend gap. This parameter is independent of the measurement method. It can be measured as the symmetry point of CT absorption and emission or by fitting either the CT band in the absorption or EQE_{PV} spectrum or in the PL or EL spectrum. Its extrapolation to 0 K coincides with the extrapolation of V_{oc} to 0 K and the activation energy of the dark current. This is in analogy with the band gaps of several inorganic solar cells. For the material blends P3HT:PCBM, APFO3:PCBM and MDMO-PPV:PCBM E_{CT} is found to be slightly temperature dependent, with E_{CT} increasing with increasing temperature.

A formula for the open-circuit voltage V_{oc} in function of the CTC properties E_{CT} , λ , and f as well as the temperature T , the short-circuit current J_{sc} , and the EL external quantum efficiency EQE_{EL} is deduced and shown to be valid for four polymer:fullerene bulk heterojunction solar cells. We show further that EQE_{EL} is not constant but depends on the injected current and thus on the number of charge carriers present in the device. This phenomenon is the origin of the ideality factor n , often used in the fitting of dark IV curves of organic solar cells.

The energetic losses between E_{CT} and qV_{oc} at room temperature and AM1.5 illumination conditions are around 0.5–0.6 eV for the investigated blends. The origin of these losses is twofold. About ~ 0.25 eV of this loss is due to unavoidable radiative losses, related to properties of the CTC formed between polymer donor and fullerene acceptor. ~ 0.35 eV is due to nonradiative losses. As these last terms represent a major loss factor for the devices investigated in this work, identification and possibly removal of the nonradiative decay paths are crucial in the future development of donor/acceptor based organic solar cells.

ACKNOWLEDGMENTS

We acknowledge the institute for the promotion of science and technology in Flanders (IWT-Vlaanderen), the Swedish Energy Agency for funding through the program Tandem, and Mats R. Andersson at Chalmers University for supplying us APFO3. Dirk Vanderzande and Wibren D. Oosterbaan are thanked for valuable discussions.

APPENDIX: DERIVATION OF EQ. (7)

In Eq. (7),

$$J_0 = \frac{q}{EQE_{EL}} \int EQE_{PV}(E) \phi_{BB}^T dE. \quad (A1)$$

We use expression (4) for EQE_{PV} ,

$$EQE_{PV}(E) = \frac{f}{E\sqrt{4\pi\lambda kT}} \exp\left(\frac{-(E_{CT} + \lambda - E)^2}{4\lambda kT}\right). \quad (A2)$$

If $E \gg kT$, the black body spectrum at temperature T can be approximated by

$$\phi_{BB}^T = \frac{2\pi}{h^3 c^2} E^2 \exp\left(-\frac{E}{kT}\right). \quad (A3)$$

We get for J_0 ,

$$J_0 = \frac{q}{EQE_{EL}} \frac{2\pi}{h^3 c^2} f \int \frac{E}{\sqrt{4\pi\lambda kT}} \times \exp\left(\frac{-(E_{CT} - E + \lambda)^2}{4\lambda kT}\right) \exp\left(\frac{-E}{kT}\right) dE. \quad (A4)$$

Collecting both exponentials in one exponential function gives

$$J_0 = \frac{q}{EQE_{EL}} \frac{2\pi}{h^3 c^2} f \int \frac{E}{\sqrt{4\pi\lambda kT}} \times \exp\left(-\frac{(E_{CT} - E + \lambda)^2 + 4\lambda E}{4\lambda kT}\right) dE. \quad (A5)$$

We will concentrate on the term within the exponential. Working out the quadrate gives

$$J_0 = \frac{q}{EQE_{EL}} \frac{2\pi}{h^3 c^2} f \int \frac{E}{\sqrt{4\pi\lambda kT}} \times \exp\left(-\frac{(E_{CT} - E)^2 + 2\lambda(E_{CT} - E) + \lambda^2 + 4\lambda E}{4\lambda kT}\right) dE. \quad (A6)$$

Rearrangement of the terms gives

$$J_0 = \frac{q}{EQE_{EL}} \frac{2\pi}{h^3 c^2} f \int \frac{E}{\sqrt{4\pi\lambda kT}} \times \exp\left(-\frac{(E_{CT} - E)^2 - 2\lambda(E_{CT} - E) + \lambda^2 + 4\lambda E_{CT}}{4\lambda kT}\right) dE. \quad (A7)$$

This can also be written as

$$J_0 = \frac{q}{EQE_{EL}} \frac{2\pi}{h^3 c^2} f \exp\left(\frac{-E_{CT}}{kT}\right) \int \frac{E}{\sqrt{4\pi\lambda kT}} \times \exp\left(\frac{-(E_{CT} - E - \lambda)^2}{4\lambda kT}\right) dE. \quad (A8)$$

The expression under the integral sign is a normalized Gaussian peaking at $E_{CT} - \lambda$, multiplied by the photon energy E . Integrating this function will give a value close to the peak of the Gaussian, i.e., $E_{CT} - \lambda$. This gives expression (8) for J_0 ,

$$J_0 \approx \frac{q}{EQE_{EL}} f \frac{2\pi}{h^3 c^2} (E_{CT} - \lambda) \exp\left(-\frac{E_{CT}}{kT}\right). \quad (A9)$$

- *Present address: Biomolecular and Organic Electronics, Center of Organic Electronics (COE), Department of Physics, Chemistry and Biology, Linköping University, 58183 Linköping, Sweden; koeva@ifm.liu.se
- ¹B. C. Thompson and J. M. J. Fréchet, *Angew. Chem., Int. Ed.* **47**, 58 (2008).
- ²G. Dennler, M. C. Scharber, and C. J. Brabec, *Adv. Mater.* **21**, 1323 (2009).
- ³S. H. Park, A. Roy, S. Beaupré, S. Cho, N. Coates, J. S. Moon, D. Moses, M. Leclerc, K. Lee, and A. J. Heeger, *Nature Photon.* **3**, 297 (2009).
- ⁴H.-Y. Chen, J. H. Hou, S. Q. Zhang, Y. Y. Liang, G. W. Yang, Y. Yang, and G. Li, *Nature Photon.* **3**, 649 (2009).
- ⁵Y. Y. Liang, Z. Xu, J. B. Xia, S.-T. Tsai, Y. Wu, G. Li, C. Ray, and L. Yu, *Adv. Mater.* (to be published).
- ⁶M. C. Scharber, D. Muhlbacher, M. Koppe, P. Denk, C. Waldauf, A. J. Heeger, and C. J. Brabec, *Adv. Mater.* **18**, 789 (2006).
- ⁷A. Gadisa, M. Svensson, M. R. Andersson, and O. Inganäs, *Appl. Phys. Lett.* **84**, 1609 (2004).
- ⁸V. D. Mihailetschi, P. W. M. Blom, J. C. Hummelen, and M. T. Rispens, *J. Appl. Phys.* **94**, 6849 (2003).
- ⁹B. P. Rand, D. P. Burk, and S. R. Forrest, *Phys. Rev. B* **75**, 115327 (2007).
- ¹⁰K. Vandewal, K. Tvingstedt, A. Gadisa, O. Inganäs, and J. V. Manca, *Nat. Mater.* **8**, 904 (2009).
- ¹¹W. Shockley and H. Queisser, *J. Appl. Phys.* **32**, 510 (1961).
- ¹²U. Rau, *Phys. Rev. B* **76**, 085303 (2007).
- ¹³L. Goris, A. Poruba, L. Hod'áková, M. Vanecek, K. Haenen, M. Nesladek, P. Wagner, D. Vanderzande, L. D. Schepper, and J. V. Manca, *Appl. Phys. Lett.* **88**, 052113 (2006).
- ¹⁴J. J. Benson-Smith, L. Goris, K. Vandewal, K. Haenen, J. V. Manca, D. Vanderzande, D. D. C. Bradley, and J. Nelson, *Adv. Funct. Mater.* **17**, 451 (2007).
- ¹⁵M. A. Loi, S. Toffanin, M. Muccini, M. Forster, U. Scherf, and M. Scharber, *Adv. Funct. Mater.* **17**, 2111 (2007).
- ¹⁶M. Hallermann, S. Haneder, and E. D. Como, *Appl. Phys. Lett.* **93**, 053307 (2008).
- ¹⁷T. Drori, C. X. Sheng, A. Ndobe, S. Singh, J. Holt, and Z. V. Vardeny, *Phys. Rev. Lett.* **101**, 037401 (2008).
- ¹⁸K. Vandewal, A. Gadisa, W. D. Oosterbaan, S. Bertho, F. Banishoeib, I. V. Severen, L. Lutsen, T. J. Cleij, D. Vanderzande, and J. V. Manca, *Adv. Funct. Mater.* **18**, 2064 (2008).
- ¹⁹D. Veldman, O. Ipek, S. C. J. Meskers, J. Sweelssen, M. M. Koetse, S. C. Veenstra, J. M. Kroon, S. S. van Bavel, J. Loos, and R. A. J. Janssen, *J. Am. Chem. Soc.* **130**, 7721 (2008).
- ²⁰Y. Zhou, K. Tvingstedt, F. Zhang, C. Du, W.-X. Ni, M. R. Andersson, and O. Inganäs, *Adv. Funct. Mater.* **19**, 3293 (2009).
- ²¹K. Tvingstedt, K. Vandewal, A. Gadisa, F. Zhang, J. V. Manca, and O. Inganäs, *J. Am. Chem. Soc.* **131**, 11819 (2009).
- ²²D. Veldman, S. C. J. Meskers, and R. A. J. Janssen, *Adv. Funct. Mater.* **19**, 1939 (2009).
- ²³P. Panda, D. Veldman, J. Sweelssen, J. J. A. M. Bastiaansen, B. M. W. Langeveld-Voss, and S. C. J. Meskers, *J. Phys. Chem. B* **111**, 5076 (2007).
- ²⁴M. D. Perez, C. Borek, S. R. Forrest, and M. E. Thompson, *J. Am. Chem. Soc.* **131**, 9281 (2009).
- ²⁵W. J. Potscavage, A. Sharma, and B. Kippelen, *Acc. Chem. Res.* **42**, 1758 (2009).
- ²⁶V. Dyakonov, *Appl. Phys. A: Mater. Sci. Process.* **79**, 21 (2004).
- ²⁷R. A. Marcus, *J. Phys. Chem.* **93**, 3078 (1989).
- ²⁸I. R. Gould, D. Noukakis, L. Gomez-Jahn, R. H. Young, J. L. Goodman, and S. Farid, *Chem. Phys.* **176**, 439 (1993).
- ²⁹N. S. Sariciftci, *Primary Photoexcitations in Conjugated Polymers: Molecular Exciton Versus Semiconductor Band Model* (World Scientific Publishing Company, Singapore, 1997).
- ³⁰L. Goris, K. Haenen, M. Nesladek, P. Wagner, D. Vanderzande, L. D. Schepper, J. D'Haen, L. Lutsen, and J. V. Manca, *J. Mater. Sci.* **40**, 1413 (2005).
- ³¹C. G. Shuttle, A. Maurano, R. Hamilton, B. O'Regan, J. C. de Mello, and J. R. Durrant, *Appl. Phys. Lett.* **93**, 183501 (2008).
- ³²C. Waldauf, M. C. Scharber, P. Schilinsky, J. A. Hauch, and C. J. Brabec, *J. Appl. Phys.* **99**, 104503 (2006).
- ³³W. J. Potscavage, S. Yoo, and B. Kippelen, *Appl. Phys. Lett.* **93**, 193308 (2008).
- ³⁴K. Kanemoto, I. Akai, H. Hashimoto, T. Karasawa, N. Negishi, and Y. Aso, *Phys. Status Solidi C* **6**, 193 (2009).
- ³⁵G. Wantz, L. Hirsch, N. Huby, L. Vignau, A. S. Barrière, and J. P. Parneix, *J. Appl. Phys.* **97**, 034505 (2005).
- ³⁶M. O. Osotov, V. V. Bruevich, and D. Y. Paraschuk, *J. Chem. Phys.* **131**, 094906 (2009).
- ³⁷M. A. Green, *Prog. Photovoltaics* **11**, 333 (2003).
- ³⁸C. Deibel, A. Baumann, and V. Dyakonov, *Appl. Phys. Lett.* **93**, 163303 (2008).
- ³⁹C. Shuttle, B. O'Regan, A. Ballantyne, J. Nelson, D. Bradley, J. D. Mello, and J. Durrant, *Appl. Phys. Lett.* **92**, 093311 (2008).
- ⁴⁰C. G. Shuttle, B. O'Regan, A. M. Ballantyne, J. Nelson, D. D. C. Bradley, and J. R. Durrant, *Phys. Rev. B* **78**, 113201 (2008).
- ⁴¹G. Juška, K. Genevičius, N. Nekrašas, G. Sliužys, and G. Dennler, *Appl. Phys. Lett.* **93**, 143303 (2008).
- ⁴²J. L. Bredas, J. E. Norton, J. Cornil, and V. Coropceanu, *Acc. Chem. Res.* **42**, 1691 (2009).